HHS Public Access

Author manuscript

Cancer Immunol Res. Author manuscript; available in PMC 2020 March 01.

Published in final edited form as:

Cancer Immunol Res. 2019 September ; 7(9): 1497–1510. doi:10.1158/2326-6066.CIR-18-0489.

Immune checkpoint protein VISTA regulates antitumor immunity by controlling myeloid cell–mediated inflammation and immunosuppression

Wenwen Xu[1], **Juan Dong**[2], **Yongwei Zheng**[1,5], **Juan Zhou**[1,7], **Ying Yuan**[1,8], **Hieu Minh Ta**[2], **Halli E. Miller**[1], **Michael Olson**[1], **Kamalakannan Rajasekaran**[5,9], **Marc S. Ernstoff**[6], **Demin Wang**[1,5], **Subramaniam Malarkannan**[1,3,4,5], **Li Wang**[2]

[1]Department of Microbiology and Immunology, Milwaukee, WI, 53226.

[2]Department of Translational Hematology and Oncology Research, Cleveland Clinic Foundation, 9500 Euclid Avenue, Cleveland, OH

[3]Department of Medicine, Milwaukee, WI, 53226.

[4]Department of Pediatrics, Medical College of Wisconsin, Milwaukee, WI, 53226.

[5]Department of Blood Research Institute, Milwaukee, WI, 53226.

[6]Roswell Park Cancer Institute, Elm & Carlton Streets, Buffalo, NY 14263.

[7]Department of Immunology, Children's Hospital of Chongqing Medical University, 136 Zhongshan Second Road, Yuzhong District, Chongqing, P.R. China.

[8] Current address: Shanghai University of Traditional Chinese Medicine, College of Pharmacy, Shanghai 201203, P.R.China.

[9] Current address: Genentech Inc, South San Francisco, CA 94080

Abstract

Immune checkpoint protein V-domain immunoglobulin suppressor of T-cell activation (VISTA) controls antitumor immunity and is a valuable target for cancer immunotherapy. This study identified a role of VISTA in regulating Toll-like receptor (TLR) signaling in myeloid cells and controlling myeloid cell–mediated inflammation and immunosuppression. VISTA modulated the polyubiquitination and protein expression of TRAF6. Consequently, VISTA dampened TLR-mediated activation of MAPK/AP-1 and IKK/NF-κB signaling cascades. At cellular levels, VISTA regulated the effector functions of myeloid-derived suppressor cells (MDSCs) and tolerogenic DC subsets. Blocking VISTA augmented their ability to produce proinflammatory mediators and diminished their T cell–suppressive functions. These myeloid cell–dependent effects resulted in a

Correspondence: Li Lily Wang, PhD, Associate Staff, Department of Translational Hematology & Oncology Research, Cleveland Clinic Foundation, NE5-217, Lerner Research Building, 2111 East 96th Street, Cleveland, OH 44195, wangl9@ccf.org; Phone: 216-445-0116; Fax: 216-636-2498.

Author contribution and Conflict-of-Interest Statements

L.W. designed and supervised this research project, analyzed data and wrote the manuscript. D.W., M.S.E., and S.M. provided reagents and protocols, provided consultation, and edited the manuscript. W.X., J.D., Y.Y., Y.Z., K.R., H.M., M.O., and J.Z. performed experiments and analyzed data. H.M. edited the manuscript. Dr. Wang has been involved with the commercial development of VISTA with ImmuNext Inc Corporation (Lebanon, NH). The other authors have no conflict of interests.

stimulatory tumor microenvironment (TME) that promoted T-cell infiltration and activation. We conclude that VISTA is a critical myeloid cell–intrinsic immune checkpoint protein and that the reprogramming of tolerogenic myeloid cells following VISTA blockade promotes the development of T cell–mediated antitumor immunity.

Keywords

Immune checkpoint protein; VISTA; myeloid-derived suppressor cells; inflammatory cytokine; immunotherapy

Introduction

The B7 family of immune checkpoint receptors are valuable targets for cancer immunotherapy. Antibodies targeting two B7 family co-inhibitory receptors CTLA-4 and PD-1 have elicited durable clinical outcomes in previously refractory cancer types, and are considered a breakthrough therapy for cancer (1,2). Despite this success, the response rate following CTLA-4, PD-L1, or PD-1-blocking monoclonal antibody (mAb) therapies is generally less than 30%, indicating that additional nonredundant immune checkpoint pathways hamper antitumor immunity (2).

VISTA (gene *Vsir*, RIKEN cDNA 4632428N05, also known as Gi24, Dies-1, PD-1H, and DD1α) stands for V-domain immunoglobulin suppressor of T-cell activation, and is an inhibitory B7 family immune checkpoint molecule (3,4). VISTA is constitutively expressed on multiple immune cell types such as $CD11b^+$ myeloid cells, naïve $CD4^+$ and $CD8^+$ T cells, $Foxp3^+CD4^+$ regulatory T cells, and TCRγδ T cells. Studies from our group and others have shown that VISTA controls T cell–mediated autoimmunity and antitumor immunity (3,5). Although other immune checkpoint regulators like CTLA-4 and PD-L1/PD-1 control T-cell activation by recruiting SHP1/2, which antagonizes proximal TCR signaling (6,7), VISTA plays a broader role in regulating both myeloid cell–mediated and T cell–mediated immune responses (4). Our previous studies in a murine model of psoriasiform inflammation show that VISTA inhibits TLR7-induced IL23 production in myeloid DCs and dampens the IL17 production in TCRγδ T cells (8). VISTA expressed on myeloid antigen-presenting cells (APCs) engages an unidentified inhibitory receptor on $CD4^+$ and $CD8^+$ T cells and suppresses their proliferation and cytokine production (3). VISTA expressed on $CD4^+$ T cells also limits T-cell activation in a T cell–intrinsic manner (9).

VISTA knockout (KO, $Vsir^{-/-}$) mice demonstrate the loss of T cell–mediated peripheral tolerance and develop inflammatory phenotypes in multiple organs (10). When bred onto an autoimmune-prone background, VISTA deficiency accelerates disease development in the experimental autoimmune encephalomyelitis (EAE) model of multiple sclerosis and the *sle1.sle3* model of lupus (10,11).

The critical role of VISTA in regulating antitumor immunity has been demonstrated by genetic deletion of VISTA gene (*Vsir*) or treatment with a VISTA-blocking mAb (4,10,12,13). Blocking VISTA deters tumor growth in multiple preclinical models (10,12),

and use of a VISTA-blocking mAb further synergizes with either the PD-L1-blocking mAb or a Toll-like receptor (TLR) agonistic peptide vaccine and CD40-specific agonistic mAb to optimally control tumor growth and achieve long-term survival (12,13). The mechanism of synergy has been attributed to the role of VISTA in directly inhibiting TCR signaling and T-cell activation (13). Whether or not VISTA regulates the activation of myeloid cells that indirectly control tumor-specific T-cell responses has not been elucidated.

This study uncovered a function of VISTA in regulating the TLR/TRAF6-mediated signaling axis and the effector function in myeloid cells. Blocking VISTA together with a TLR agonistic vaccine abolished the suppressive functions of MDSCs and tumorigenic DCs and augmented the production of proinflammatory cytokines. These effects collectively led to a T cell–permissive tumor microenvironment (TME) that facilitated tumor rejection. The reprogramming of tumor-associated myeloid cells contributes to the protective antitumor immunity following VISTA inhibition.

Materials and Methods

EXPERIMENTAL MODEL AND SUBJECT DETAILS

Mice—C57BL/6 (wild-type, WT) mice were purchased from Charles River Laboratories. *Vsir*$^{-/-}$ mice on a fully backcrossed C57BL/6 background were obtained from Mutant Mouse Regional Resource Centers (www.mmrrc.org; stock no. 031656-UCD) (10,13). *Myd88*$^{-/-}$ mice were purchased from the Jackson Laboratory (Bar Harbor, ME). OT-I CD8^{+} TCR transgenic mice were purchased from Jax (stock # 003831). Animals were maintained in a specific pathogen-free facility at the Medical College of Wisconsin, Milwaukee, WI. All animal protocols were approved by the Institutional Animal Care and Use Committee of the Medical College of Wisconsin. All methods were performed in accordance with the relevant guidelines and regulations.

Cell lines—B16-BL6 murine melanoma cells were cultured in RPMI-1640 supplemented with 10% FBS, 0.1% β-mercaptoethanol, and penicillin (100 U/mL) /streptomycin (100 μg/ml). B16-BL6 (female origin) was originally obtained from I. Fidler (MD Anderson Cancer Center) and were verified by *in vivo* growth in syngeneic mice and their expression of melanoma antigens TRP1, TRP2, and gp100, but have not been authenticated further by other methods. Murine thymoma EG7 (female origin), human THP-1 (male origin) monocytes, and human HEK293T cells were authenticated and obtained from ATCC and were cultured in the same RPMI-1640 media as above. To generate a VISTA-overexpressing THP-1 cell line, THP-1 cells were transduced with lentivirus carrying human VISTA gene that was cloned into a lentiviral vector pFLRcmv-FH-puro. Transduced cells were stained with VISTA-specific mAb and FACS sorted to homogeneity. Lentivirus carrying the empty vector was used to generate the control THP-1 cell line. All cell lines were used at less than five passages and after short-term (less than one week) culture time. Cell lines were tested for mycoplasma contamination every 5–6 months, using MycoAlert™ Mycoplasma Detection Kit (Lonza Inc, Allendale, NJ).

Examination of TLR-mediated signaling—WT or *Vsir*$^{-/-}$ mice (two to three of each genotype) were treated with 3 mL 3% thioglycolate broth (Cat# DF0430–17-1,

ThermoFisher Scientific Inc, Waltham, MA). Peritoneal macrophages were harvested from peritoneal lavage on day +4 following thioglycollate injection. Cells were rested in RPMI media supplemented with 1% FBS, 2 mM L-glutamine, and 50 μM β-mercaptoethanol for one hour before stimulation with TLR agonists including LPS (1 μg/mL), CpG (1μg/mL; OND1826), Poly (I:C)(25 μg/mL), Pam3cys4 (10 μg/mL), and R848 (5 μg/mL). All TLR agonists were purchased from InvivoGen (San Diego, CA). mRNA samples were collected after 3 hours using RNeasy mini kit (Qiagen, Hilden, Germany) following manufacture instructions. Expression of genes *Il12p35, Il12p40*, and *Il6* were examined by real-time qRT-PCR as described below. Culture supernatants were harvested after 5 hours and examined by ELISA to assess the level of cytokines IL6, IL12p40, GM-CSF, IFNγ, MIP-1α, MIP-1β as described below. To determine the effect of TNFα, macrophages were stimulated with CpG (1 μg/mL) in the presence of a TNF receptor-specific blocking mAb (Bio X cell Inc, Lebanon, NH) or isotype control IgG (25 μg/ml) for 6 hours before culture supernatants were harvested and examined by ELISA.

For measuring TLR-mediated signaling, macrophages or THP-1 cells were stimulated with Pam3 or CpG respectively for 0, 15, and 30 minutes. When indicated, cells were pre-treated with MG132 (10 μg/mL; Sigma-Aldrich, St Louis, MO) or DMSO vehicle control for 30 minutes before TLR stimulation. Cells were lysed in RIPA buffer (50 mM Tris pH 7.4, 150 mM NaCl, 1.0% NP-40, 0.5% deoxycholic acid, 0.1% SDS, 1 mM EDTA, 1 mM EGTA, 5 mM sodium pyrophosphate, 50 mM NaF, 10 mM β-glycerophosphate) supplemented with 1x Halt™ protease and phosphatase inhibitors cocktail (Cat #78442, ThermoFisher Scientific Inc, Waltham, MA) at indicated time points. Phosphorylated and total levels of proteins including Jnk1/2, Erk1/2, p38, IKB, IKKα/β were examined by Western blotting as described below.

For denaturing immunoprecipitation (IP) of TRAF6, WT or *Vsir*$^{-/-}$ macrophages were lysed in lysis buffer (1% NP-40, 50 mM Tris-HCl, pH 7.5, 150 mM NaCl, 5 mM EDTA) containing 1% SDS and denatured by heating for 5 minutes. Lysates (200 μg) were diluted with SDS-free lysis buffer until the concentration of SDS reached 0.1%. TRAF6 was immunoprecipitated using a mouse monoclonal antibody (4 μg for 200 μg lysates) (sc-8409) from Santa Cruz Biotechnology Inc (Dallas, TX) and 20 μL protein G agarose beads (MilliporeSigma Inc, Burlington, MA). Bound proteins were eluted using 1x SDS sample buffer and analyzed by Western blotting as described below. For HEK293T cells that were transfected with HA-tagged mutant ubiquitin and VISTA-expressing or control vectors, cells were stimulated with R848 (10 μg/mL) for 15 minutes before lysed in the denaturing IP buffer and TRAF6 was immunoprecipitated as described above.

Electrophoretic mobility shift assays (EMSA) were used to measure the DNA binding activity of transcription factors AP-1 and NF-κB, using radiolabeled DNA probes as previously described (15). Briefly, WT or *Vsir*$^{-/-}$ macrophages (2–3 × 10^6 cells) were lysed in 50 μL buffer containing 20 mM HEPES pH 7.9, 350 mM NaCl, 1 mM $MgCl_2$, 0.5 mM EDTA, 0.5 mM DTT, 20% glycerol, 1% NP-40. Cell lysates (3 μL) were incubated with [32P]-labeled NF-κB probe (cat# SC-2505) or AP-1 probe (cat# SC-2501; 25,000 cpm per reaction) (Santa Cruz Biotechnology) for 15 minutes at room temperature and then resolved on a 4% polyacrylamide gel.

Real-time Quantitative RT-PCR (qRT-PCR)—Single cell suspensions of tumor-draining lymph nodes (LNs) were obtained by passing cells through 70 um cell strainers. For peritoneal macrophages, cells (1–2 million) were stimulated with CpG (1 μg/mL) or R848 (5 μg/mL) for 3 hours before RNA isolation. Total RNA of LN cells or macrophages was prepared using the RNeasy Kit (Qiagen, Hilden, Germany). 1 μg of total RNA was reverse transcribed in 50 μΛ of TaqMan reverse transcription reagents (Applied Biosystems) using random hexamer primers and according to manufacturer's instructions. 10 ng cDNA and 1 uM primers were used in a 20 μL PCR reaction with SYBR Green Supermix (Bio-Rad). PCR reaction was performed in the Bio-Rad iQ5 Real-Time PCR System (Bio-Rad, Hercules, CA). Each sample have triplicate replication and $2^{-\Delta\Delta CT}$ method was used to determine gene expression. Expression of the target genes was normalized to 18s and displayed as fold change relative to the WT sample. Primers were purchased from Integrated DNA Technologies (Coralville, Iowa).

Primer sequences are described in the following: *Il23-p19* (forward: CCAGCAGCTCTCTCGGAATC; reverse: TCATATGTCCCGCTGGTGC)*; IL12 p40* (forward: ACA GCA CCA GCT TCT TCA TCA; reverse TCT TCA AAG GCT TCA TCT GCA A); *Ifnb* (forward: CAGCCCTCTCCATCAACTATAAG; reverse: TCTCCGTCATCTCCATAGGG); *Il6* (forward: GCAGAAAAAGGCAAAGAATC; reverse: CTACATTTGCCGAAGAGC)*; Tnfa* (forward: AGGCAGTCAGATCATCTTC; reverse: TTATCTCTCAGCTCCACG); 18s RNA (forward: AACCCGTTGAACCCCATT; reverse: CCATCCAATCGGTAGTAGCG).

Western blotting—For western blotting, antibodies specific for K63-linked and K48-linked polyubiquitin chains, p-Erk1/2 (Thr202/Tyr204), Erk1/2, p-Jnk1/2 (Thr183/Tyr185), Jnk1/2, p-p38, p38, p-IKKα/β, IKKα/β, p-NF-κBp65, NF-κBp65, IκB, TRAF6, pTAK1(Thr184/187), and TAK1 were purchased from Cell Signaling Technology (Boston, MA). Antibodies specific for actin were purchased from Santa Cruz Biotechnology Inc (Dallas, TX). VISTA-blocking mAb was as described previously (12). HA-tagged mutant ubiquitin pRK5-HA-Ubiquitin-K63 and pRK5-HA-Ubiquitin-K48 were a gift from Ted Dawson (Addgene plasmid #17606 and #17065) (14). All primary antibodies were used at 1:1000 dilution. HRP-conjugated secondary antibodies (1:5000 dilution; (Jackson ImmunoResearch Laboratories, West Grove, PA).

THP-1 cells or peritoneal macrophages ($5–10 \times 10^6$) stimulated with relevant TLR agonists were lysed in RIPA buffer (50 mM Tris pH 7.4, 150 mM NaCl, 1.0% NP-40, 0.5% deoxycholic acid, 0.1% SDS, 1 mM EDTA, 1 mM EGTA, 5 mM sodium pyrophosphate, 50 mM NaF, 10 mM - β glycerophosphate) supplemented with Halt™ Protease and Phosphatase Inhibitor Cocktail (100X; ThermoFisher Scientific Inc, Waltham, MA) at indicated time points. Total lysates were cleared by spinning at 12,000 rpm for 10 minutes. 20 μg lysates were subjected to SDS-PAGE and Western blotting. For detecting TRAF6 in WT or *Vsir*$^{-/-}$macrophages and HEK293T cells, 50% of the eluates from the denaturing IP (described above) were used for SDS-PAGE and Western blotting.

All primary antibodies were used at 1:1000 dilution. Appropriate secondary antibodies were used at 1:5000 dilution. Proteins were detected using Clarity™ Western ECL Substrate (Bio-

Rad, Hercules, CA) and X-ray films. Results were scanned using a digital scanner at 600 dpi resolution and quantified using Image J software.

ELISAs—For ELISA analyses, culture supernatants from peritoneal macrophages were diluted 5-fold, homogenized tumor tissues were diluted 5-fold, plasma samples were diluted 5-fold, culture supernatants from MDSC suppression assays were diluted 50-fold. All dilutions were using PBS with 2% BSA as diluent. ELISA kits for detecting murine IL12p40, IL12p70, IL23p19, IL6, TNFα, IFNβ, IL27, GM-CSF, MIP-1α, MIP-1β, CCL4, CCL5, CXCL9, and CXCL10 were purchased from BioLegend Inc (San Diego, CA). OD450 values were read using Typhoon 9400.

Murine tumor models, vaccine treatments, and examination of cytokines in tumor tissues—EG7 (150,000) or B16-BL6 (30,000) tumor cells were inoculated intradermally on the right flanks of female and male C57BL6 mice of 7–9 weeks of age. A similar number of female and male mice were pooled and allocated for each experimental group (n=10). The peptide vaccine mixture consists of CpG (ODN1826, 50 μg), R848 (100 μg), melanocyte antigen peptide TRP1 (106–130; 50 μg), and a mutated TRP2 peptide DeltaV-TRP2 (180–188; 50 μg) dissolved in PBS (16). All peptides were synthesized by Atlantic Peptides Inc (Lewisburg, PA). The vaccine mixture was injected subcutaneously on day +3 following tumor inoculation. Tumor-bearing mice were treated subcutaneously with VISTA-specific mAbs or hamster control IgG (200 μg per injection for both) every 2–3 days until the analytical endpoint, or for 5 weeks if mice remained tumor-free. Tumor size was measured with a caliper every 2–3 days.

For measuring cytokines within tumor tissues, mice bearing tumors 5–6 mm in diameter were treated with CpG (20 μg), R848 (50 μg), and VISTA-specific mAb or control IgG as described above. Tumor tissues were harvested after 3 hours and homogenized using the QIAGEN tissue homogenizer in buffer containing 1x PBS, 0.1% Tween 20, and 1x Halt™ protease inhibitor cocktail (ThermoFisher Scientific Inc, Waltham, MA). The homogenates were cleared by centrifugation at 10,000 × *g* for 20 minutes. Cytokines and chemokines in the supernatant were detected by ELISA as described above. For detecting cytokines in blood, heparinized blood samples were harvested via cardiac puncture and centrifuged at 2500 rpm for 10 minutes. Plasma was collected and also examined by ELISA.

Examination of tumor-associated myeloid cells—Thirty to forty B16-BL6 tumors (7–8 mm in diameter) were harvested from untreated tumor-bearing C57BL6 WT mice. Tumors were pooled, cut into smaller pieces, and digested for 20 minutes at 37° C in RPMI buffer containing Liberase™ TL (150 μg/mL) and DNase I (120 μg/mL) (Sigma-Aldrich, St Louis, MO). Single-cell suspensions were generated by passing cells through 70 μm cell strainers. Myeloid cells, including polymorphonuclear PMN-MDSCs ($CD11b^+CD11C^-LY6C^{int}$ $LY6G^+$), monocytic M-MDSCs ($CD11b^+CD11C^-LY6C^{hi}LY6G^-$), myeloid conventional cDCs ($CD11b^+CD11C^+MHCII^+LY6C^-F4/80^-CD103^-$), inflammatory (Inf)-DCs ($CD11b^+CD11C^+MHCII^+LY6C^+$ $LY6G^-FcεRI^+$), and $CD103^+$ DCs ($CD103^+CD11C^+MHCII^+$ $F4/80^-$) were purified from dissociated tumor tissues by FACS sorting using BD FACSAria™ II, with 99% purity.

To test TLR-mediated cytokine production, purified myeloid cell subsets (10,000 cells) were stimulated with TLR9 agonist CpG (1 μg/mL) in the presence of VISTA-blocking mAb (20 μg/mL) or isotype control IgG (20 μg/mL) as indicated. Culture supernatants were harvested after 24 hours. Secreted cytokines (IL12p40, IL6, and TNFα) were quantified by ELISA as described above.

For testing the T cell-suppressive function of MDSCs, sorted myeloid cDCs, and Inf-DCs (10,000) were cocultured with 30,000 whole splenocytes from OT-I $CD8^+$ TCR transgenic mice together with ovalbumin peptide 257–264 (1 μg/mL) (Genscript Inc, Piscataway, NJ), CpG (1 μg/ml), and VISTA-blocking mAb or control IgG (20 μg/mL) as indicated. Culture supernatants were harvested after 48 hours and secreted IFNγ was quantified by ELISA. For testing the T cell-stimulatory function of $CD103^+$ DCs, sorted $CD103^+$ DCs (10,000) were cocultured with 30,000 purified OT-I $CD8^+$ T cells, ovalbumin peptide 257–264 (1 μg/mL), CpG (1 μg/mL), and VISTA-blocking mAb or control IgG (20 μg/mL) as indicated. Culture supernatants were harvested after 48 hours and secreted IFNγ was quantified by ELISA.

Flow Cytometry and data analysis—For flow cytometry, antibodies specific for CD4 (GK1.5), CD8 (53–6.7), CD16/CD32, and IFNγ (XMG1.2) were purchased from BioLegend (San Diego, CA). Single-cell suspensions tumor tissues and spleens were stained with lineage-specific antibodies (CD4, CD8, CD11b, CD11c, Ly6C, Ly6G, MHCII, F4/80, and FcεRI) to identify $CD4^+$ and $CD8^+$ T cells and myeloid cell populations. To detect intracellular cytokines in T cells, single-cell suspensions of tumor tissues (2–3 million) were stimulated for 5 hours in RPMI medium containing PMA (50 μg/mL), ionomycin (1 μg/mL), 10% FBS, 2 mM L-glutamine, 50 μM 2-mercaptoethanol, 1% penicillin-streptavidin, 1x monensin, 1x Brefeldin A (BioLegend, San Diego, CA). Cells were stained with LIVE/DEAD™ Fixable Violet Dead Cell Stain Kit first (ThermoFisher Scientific Inc, Waltham, MA), then stained with T-cell lineage markers in the presence of pan CD16/CD32 blocking antibody before fixation with 1% paraformaldehyde, then permeabilized with 0.5% saponin and stained for intracellular IFNγ. Cells were analyzed on a LSR II flow cytometer (BD Biosciences, San Jose, CA). Data were analyzed with FlowJo version 9.9.6 analysis software (Tree Star, San Carlos, CA).

Graphs and statistical analysis—All graphs and statistical analysis were generated using Prism 7 (GraphPad Software, Inc., San Diego, CA). Unpaired two-tailed t-tests were used for comparing WT and *Vsir*$^{-/-}$ cells or mice, or comparing treatments using VISTA-blocking mAb or control IgG. Survival differences of tumor-bearing mice were assessed using Kaplan-Meier curves and analyzed by log-rank testing. A P-value less than 0.05 was considered as statistically significant. *$p<0.05$; **$p<0.025$; ***$p<0.005$; ****$p<0.0001$.

Results

Absence of VISTA augments TLR-mediated proinflammatory cytokine production

TLR stimulation initiates MyD88- or TRIF-dependent signaling pathways to induce the expression of proinflammatory cytokines, chemokines, and type I interferons (17). Owing to the high expression of multiple TLRs on peritoneal macrophages, we chose this cellular system as a model to dissect the role of VISTA in regulating TLR-mediated signaling

pathways. Peritoneal macrophages were isolated from WT and *Vsir*$^{-/-}$ mice following thioglycollate treatment and stimulated *ex vivo* with TLR agonists CpG (TLR9) and R848 (TLR7)(Figure 1A–C). The expression of cytokines IL12 and IL6 were examined by real-time qRT-PCR and ELISA. CpG and R848 significantly upregulated gene expression and protein production of IL12 and IL6 in *Vsir*$^{-/-}$ macrophages (Figure 1A–B). The expression of multiple cytokines and chemokines, including GM-CSF, IFNγ, MIP-1α, and MIP-1β were also significantly increased in *Vsir*$^{-/-}$ macrophages (Figure 1C). In addition to CpG and R848, *Vsir*$^{-/-}$ macrophages were hyper-responsive towards additional TLR agonists including Pam3Cys4 (TLR2), LPS (TLR4), and poly (I:C) (TLR3)(Figure 1D).

Although the results above indicated that VISTA directly regulated TLR-mediated signaling, we wanted to assess if cell-extrinsic factors such as TNFα or additional soluble factors may have contributed to the hyper-responses of *Vsir*$^{-/-}$ cells in an autocrine manner. We first tested a TNFR-specific neutralizing mAb and found minimal effects (Supplementary Figure S1A). Next, we harvested supernatants from CpG-treated WT and *Vsir*$^{-/-}$ cell cultures (designated as WT and KO sups, respectively) and tested their effects on freshly isolated peritoneal macrophages (Supplementary Figure S1B). The residual CpG in the supernatants directly stimulated cells, and adding CpG to the culture further boosted cytokine production. Under all tested conditions, WT and KO supernatants stimulated cells to similar levels. This data supports the conclusion that the hyper-responsiveness in *Vsir*$^{-/-}$ macrophages was due to cell-intrinsic TLR signaling rather than secondary responses to soluble factors.

VISTA inhibits the activation of MAP kinases and NF-κB signaling cascades

Transcription factors AP-1 and NF-κB are critical for the gene expression of many inflammatory cytokines and chemokines (18). Previous studies have established the role of MAP kinases (MAPKs Erk1/2, Jnk1/2, and p38) in the activation of AP-1 (19,20). The activation of NF-κB requires the phosphorylation of IκB kinase IKKα/β and degradation of the inhibitor IκB (21). We, therefore, examined the activation of MAPKs/AP-1 and IKK/NF-κB signaling cascades following TLR stimulation. Cell lysates from WT and *Vsir*$^{-/-}$ macrophages were stimulated with CpG or R848. Phosphorylation of MAPKs and IKKα/β, as well as total IκB, were examined by Western blotting. Both CpG (Figure 2A) and R848 (Figure 2B) induced greater phosphorylation of Erk1/2, Jnk1/2, and p38 in *Vsir*$^{-/-}$ macrophages. Phosphorylation of IKKα/β and degradation of IκB were enhanced in *Vsir*$^{-/-}$ macrophages following CpG stimulation, but were not significantly increased following R848 stimulation.

Next, we carried out EMSA assays to measure the DNA binding activity of AP-1 and NF-κB. As shown in Figure 2C, CpG stimulation induced higher activation of AP-1 and NF-κB in *Vsir*$^{-/-}$ macrophages than in WT cells. These results indicate that VISTA inhibited TLR-mediated activation of MAPKs/AP-1 and IKK/NF-κB signaling cascades.

Previous studies show that *Vsir*$^{-/-}$ mice develop systemic tissue inflammation (10). It is possible that *Vsir*$^{-/-}$ macrophages were partially activated due to exposure to the existing tissue inflammation. To rule out this possibility and validate the cell-intrinsic role of VISTA, we examined the effects of VISTA-overexpression in THP-1 human monocyte cells. VISTA^{+} and control THP-1 cells were stimulated with TLR2 agonist Pam3Cys4 (10 μg/ml) for the

indicated time and total cell lysates were harvested and analyzed by western blotting (Figure 3). VISTA expression in THP-1 cells suppressed the phosphorylation of MAPKs (Jnk1/2, Erk1/2, and p38) (Figure 3A,C), the phosphorylation of IKKα/β and NF-κB p65, and the degradation of IκB (Figure 3B–C) following TLR2 stimulation.

VISTA controls the activation of MAPKs and NF-κB by regulating TRAF6

TLRs utilize either MyD88-dependent (TLR2/4/5/7/8/9) or TRIF-dependent (TLR3/4) signaling pathways (22). Following TLR2/4/5/7/8/9 engagement, the MyD88/IRAK1/4 complex recruits and activates the RING-domain E3 ubiquitin ligase TRAF6, which is required for the activation of MAPKs and NF-κB (22). TRAF6 also mediates the activation of NF-κB downstream of TLR3 by binding to TRIF (23). Because *Vsir*$^{-/-}$ macrophages are hyper-responsive to all TLR agonists (Figures 1–3), we hypothesized that VISTA targeted a shared signaling adaptor such as TRAF6 (24). We first examined the total protein level of TRAF6 and observed increased TRAF6 expression in freshly isolated *Vsir*$^{-/-}$ macrophages compared to WT cells (Figure 4A). Because K48-linked polyubiquitination could target proteins to proteasomes for degradation and K63-linked polyubiquitination activates TRAF6 (25), we analyzed the ubiquitination status of TRAF6 after immunoprecipitating TRAF6 under denaturing conditions (Figure 4B). Western blots showed that VISTA deletion resulted in lower K48-linked polyubiquitination and higher K63-linked polyubiquitination of TRAF6 following CpG stimulation (Figure 4B).

Next, we utilized HA-tagged mutant ubiquitin that contains only K48 (HA-Ub-K48) or K63 (HA-Ub-K63) to determine the effect of transient VISTA expression on TRAF6 ubiquitination. HEK293T cells were co-transfected with mutant ubiquitin together with a VISTA-expressing vector or empty control vector and analyzed at 24 hours post transfection (Figure 4C). Transient VISTA expression significantly augmented K48-linked polyubiquitination of TRAF6 and simultaneously decreased K63-linked polyubiquitination levels (Figure 4C).

The TAK1/TAB1/TAB2 complex is recruited to the MyD88/IRAK/TRAF6 complex by binding to the K63-polyubiquitin chains of TRAF6 and mediates the activation of Jnk1/2/AP-1 and IKKα/β/NF-κB signaling pathways (25). Consistent with the higher protein level and K63 polyubiquitination of TRAF6, phosphorylation of TAK1 at Thr$^{184/187}$ in *Vsir*$^{-/-}$ macrophages was significantly enhanced compared to WT cells following CpG stimulation (Figure 4D). Reduced protein expression of TRAF6 and diminished TAK1 activation were also seen in VISTA-expressing THP-1 cells compared to control THP-1 cells following Pam3Cys4 treatment (Figure 4E–F).

These results prompted us to test whether proteasomal inhibition reversed the inhibitory effects of VISTA. As shown in Figure 5A, pretreatment with a proteasome inhibitor MG132 effectively reversed the inhibitory effects of VISTA in THP-1 cells by rescuing the phosphorylation of Jnk1/2, Erk1/2, p38, and IKKα/β. MG132 pretreatment also enhanced TLR signaling in WT but not VISTA-deficient macrophages (Figure 5B). These results, therefore, support the conclusion that VISTA downregulates TLR-mediated signaling by promoting TRAF6 protein degradation and restricting the activation of MAPKs/AP-1 and IKKα/β/NF-κB signaling pathways.

Blocking VISTA augments the TLR/MyD88-mediated proinflammatory responses

We have previously shown that treatment with a VISTA-blocking mAb deters tumor growth in preclinical models (12). Our current study indicated that the proinflammatory responses induced by VISTA blockade promote the development of antitumor immunity. Supporting this hypothesis, treatment with the VISTA-blocking mAb led to a significant accumulation of IL12p40, IL12p70, TNFα, and IL27 in the serum of mice (Figure 6A). This cytokine response was absent in tumor-bearing MyD88 KO hosts (Figure 6B). Consistent with the lack of cytokine induction, the therapeutic efficacy of the VISTA-blocking mAb was diminished in MyD88 KO hosts (Figure 6C). These results indicated that blocking VISTA elicited an endogenous TLR/MyD88-mediated proinflammatory response that contributed to the development of antitumor immune responses.

TLR agonists are promising vaccine adjuvants for cancer therapy (26,27). We hypothesized that VISTA inhibitors would synergize with TLR-agonistic vaccines owing to an augmented proinflammatory response. We tested this hypothesis in the B16-BL6 melanoma model (Figure 6C). Mice bearing three-day established B16-BL6 tumors were treated with either VISTA-blocking mAb, or a vaccine containing TLR7/8/9 agonists (CpG and R848) and peptides derived from melanoma antigens TRP1 and TRP2, or both. Combining VISTA-blocking mAb with the TLR vaccine resulted in tumor-free long-term survival in ~50% mice, whereas either monotherapy transiently delayed tumor growth without long-lasting effects (Figure 6C). This stronger therapeutic effect correlated with significantly increased numbers of IFNγ-expressing tumor-infiltrating $CD8^+$ and $CD4^+$ T cells (Figure 6D–E).

To dissect the inflammatory TME, we examined the expression of inflammatory mediators within tumor tissues following CpG/R848 treatment (Figure 6F,H). The VISTA-blocking mAb significantly enhanced the expression of cytokines (IL12p40, IL12p70, IL23p19, IL6, IFNβ, and TNFα) and chemokines (CCL4, CCL5, CXCL9, CXCL10). To exclude the possibility that this inflammatory response may be due to additional effects of the antibody (i.e Fc receptor–mediated activation of myeloid cells), we examined WT and *Vsir*$^{-/-}$ tumor-bearing mice treated with CpG/R848 (Figure 6G,I). Consistent with the antibody treatment, *Vsir*$^{-/-}$ mice produced higher amount s of inflammatory mediators. In addition to tumor tissues, enhanced cytokine production was detected in tumor-draining lymph nodes (Supplementary Figure S2). These results indicated that VISTA blockade augments the proinflammatory responses in the periphery and within the TME, which are critical for the development of antitumor T-cell responses.

VISTA regulates the effector functions of tumor-associated myeloid cells

Tumor tissues are enriched with immunosuppressive MDSCs and dysfunctional DCs (28,29). Importantly, VISTA is expressed on tumor-associated myeloid cDCs ($CD11b^+CD11C^+$ $MHCII^+LY6C^-$), inflammatory DCs (Inf-DCs, $CD11b^+CD11C^+MHCII^+Ly6C^+Ly6G^-Fc\varepsilon RI^+$), PMN-MDSCs ($CD11b^+CD11C^-Ly6C^{int}Ly6G^+$) and M-MDSCs ($CD11b^+CD11C^-Ly6C^+Ly6G^-$), as well as on $CD103^+$ DCs (Figure 7A). This result led us to examine how VISTA directly regulated the effector function of these myeloid cell types in tumor-bearing hosts.

We first analyzed the accumulation of MDSCs and DC subsets in tumor-bearing mice treated with CpG/R848 and VISTA-blocking mAb (Figure 7B). VISTA inhibition reduced the accumulation of M-MDSCs and PMN-MDSCs and concurrently expanded Inf-DCs within tumor tissues (Figure 7B). A similar reduction of PMN-MDSCs and expansion of Inf-DCs was observed in the spleen, whereas the number of M-MDSCs in the spleen remained unaltered (Supplementary Figure S3). The number of $CD103^+$ DCs and myeloid cDCs within tumor tissues and spleen were not significantly altered.

Next, we assessed whether VISTA blockade augmented the ability of tumor-associated myeloid cells to produce immune-stimulatory cytokines, such as IL12 (30). We purified MDSCs and DC subsets from tumor tissues and examined their cytokine expression following CpG/TLR9 stimulation. Our results showed that, with the exception of PMN-MDSCs, VISTA blockade significantly augmented the expression of IL12p40 in M-MDSCs, Inf-DCs, myeloid cDCs, and $CD103^+$ DCs (Figure 7C).

In addition to cytokine production, we sought to determine whether VISTA regulated the immunosuppressive functions of tumor-associated myeloid cells. Tumor-associated MDSCs (Figure 7D–E), Inf-DCs (Figure 7F), and myeloid cDCs (Figure 7G) inhibited IFNγ production by OT-I $CD8^+$ T cells stimulated with splenic APCs. The VISTA-blocking mAb or TLR stimulation partially reversed the suppressive functions of M-MDSCs, myeloid cDCs, and Inf-DCs, whereas combined treatments maximally abolished suppression (Figure 7D–F). MyD88 KO M-MDSCs failed to respond to the VISTA-blocking mAb, thus, validating the role of MyD88 in mediating the myeloid-intrinsic function of VISTA (Figure 7D). On the other hand, PMN-MDSCs were not responsive to VISTA inhibition or TLR stimulation (Figure 7E).

In contrast to the tolerogenic tumor-infiltrating myeloid cDCs and Inf-DCs, Batf3-dependent $CD103^+$ DCs are the most potent cross-presenting DCs that prime CTLs at the tumor site (29,31,32). We showed that VISTA was expressed on $CD103^+$ DCs (Figure 7A) and treatment with VISTA-blocking mAb significantly augmented IFNγ production from purified OT-I $CD8^+$ T cells cocultured with $CD103^+$ DCs, whereas CpG treatment had only minimal impact (Figure 7H). Combining VISTA blockade with CpG treatment led to optimal T-cell activation and IFNγ production (Figure 7H). Together, these results indicated that blocking VISTA promotes the development of antitumor immunity by reprogramming tumor-associated tolerogenic MDSCs and DCs.

Discussion

Previous studies have shown that VISTA is expressed on myeloid cells at steady state and in tumor-bearing hosts, but the myeloid-intrinsic functions of VISTA have not been elucidated (3,12,33,34). This study demonstrated that VISTA downregulated the TLR/TRAF6/TAK1 signaling pathway by modulating the polyubiquitination and protein expression of TRAF6. At cellular levels, VISTA regulated the effector functions of MDSCs and DC subsets. Targeting VISTA in tumor-associated myeloid cells induced inflammatory cytokines and promoted antitumor T-cell responses.

TLRs expressed on DCs and other APCs maintain antitumor immuno-surveillance by recognizing endogenous danger-associated molecular patterns (DAMPs) derived from commensal/invading microbes or necrotic tumors (35,36). Our study showed that in the absence of a TLR agonistic vaccine, the efficacy of the VISTA-blocking mAb relied upon endogenous TLR/MyD88-mediated signaling and correlated with the production of immune-stimulatory cytokines such as IL12, IL27, and TNFα. Thus, VISTA inhibited antitumor immuno-surveillance at the steady state.

Synthetic TLR agonists such as imiquimod (a TLR7 agonist) and PF-3512676 (CpG ODN for TLR9) are promising vaccine adjuvants (27,37). We showed that in conjunction with the TLR7/8/9 agonistic vaccine, VISTA blockade augmented the expression of chemokines (CXCL9/10, CCL4/5) and cytokines (IFNβ, IL12, IL27, IL23, IL6, and TNFα) within tumor tissues. Intratumor CXCL9/10 and CCL4/5 are critical for recruiting Th1 $CD4^+$ T cells and $CD8^+$ cytotoxic T cells and are associated with better clinical outcomes in various cancer types (38–40). Although IL12, IL27, TNFα, and IFNβ play well-established roles in promoting antitumor T-cell responses (30,41,42), IL6 impairs antitumor immunity by inducing STAT3 activation in tumor cells and MDSCs (43). IL23 can both promote and inhibit tumor growth, depending upon the stage of tumor development (44). It remains to be determined whether neutralizing IL6 and IL23 will improve the antitumor efficacy of VISTA inhibitors and reduce immune-related adverse events (irAEs).

Tumor tissues are enriched with dysfunctional and immunosuppressive MDSCs and myeloid DCs (29,45). MDSCs utilize diverse mechanisms such as the production of reactive oxygen species (ROS), nitric oxide (NO), and the secretion of arginase I, IL10, and TGFβ to inhibit T-cell responses (45). Tumor-associated myeloid DCs impair T-cell activation by expressing PD-L1 or secreting soluble mediators such as galectin-1 (46,47), and the frequencies of circulating MDSCs have been correlated with resistance to ipilimumab therapy in melanoma patients (45,48). Myeloid-inflamed TME profile associates with poor clinical outcomes in pancreatic cancer and head and neck cancer following GVAX vaccine therapy (49). Therefore, effective strategies that reduce the accumulation and suppressive functions of tumorigenic myeloid cells are urgently needed.

Our study showed that VISTA was an immune checkpoint protein that regulated the immunosuppressive functions of tumor-associated myeloid cells. Blocking VISTA together with TLR stimulation abolished the suppressive function of M-MDSCs and myeloid DCs and induced IL12 production. These myeloid cell–dependent effects converted the immunosuppressive TME into a T cell–stimulatory one that may sensitize tumors to additional immunotherapies. Supporting this notion, we have previously shown that blocking VISTA synergizes with PD-L1 inhibitors in murine tumor models (13).

In contrast to M-MDSCs, the suppressive function of PMN-MDSCs was not reversed by the VISTA-blocking mAb, despite high VISTA expression on these cells. This result indicated that tumors enriched with PMN-MDSCs may be resistant to VISTA-targeted inhibitors. Previous studies have identified approaches to reduce the accumulation and suppressive functions of PMN-MDSCs, including treatment with sildenafil (50), gemcitabine (51), inhibitors of DNA methyltransferase or histone deacetylase (52), and PI3Kδ/γ inhibitor

(53). However, it remains to be determined if combining VISTA inhibitors with these reagents will maximally block both PMN-MDSCs, M-MDSCs, and other tumorigenic myeloid DCs, thereby achieving optimal therapeutic outcomes.

In conclusion, this study established VISTA as an immune checkpoint protein that regulates the functions of myeloid cells and that myeloid cell activation contributes to the overall antitumor mechanisms of VISTA inhibitors. Unlike VISTA, immune checkpoint proteins CTLA-4 and PD-1 do not directly regulate the function of myeloid cells (28). Targeting VISTA may be a valuable approach for patients resistant to the existing immune checkpoint inhibitors. Results from this study provide insights for monitoring myeloid cell–dependent inflammatory responses that precede T cell–mediated antitumor responses following VISTA-targeted therapies.

Supplementary Material

Refer to Web version on PubMed Central for supplementary material.

Acknowledgments

This study was supported by research funding from NCI R01 CA164225 (L.W.), Advancing A Healthier Wisconsin Research and Education Program (AHW REP) fund (L.W.), the Office of the Assistant Secretary of Defense for Health Affairs through the Peer Reviewed Cancer Research Program under Award No. W81XWH-14-1-0587 (L.W.), Worldwide Cancer Research Foundation (UK) research grant 16-1161 (L.W.). This work is also supported by the Uehara Foundation (Y.I.), NIH R01 AI102893 (S.M.), NCI R01 CA179363 (S.M.), Nicholas Family Foundation (S.M.), and Gardetto Family (S.M.), PO1 CA 206980 and P30 CA 016056 (M.S.E), and NIH grants AI079087 (D.W.), HL130724 (D.W.) and Gardetto Family (D.W.).

References

1. Sharma P, Allison JP. 2015 The future of immune checkpoint therapy. Science 348: 56–61 [PubMed: 25838373]
2. Postow MA, Callahan MK, Wolchok JD. 2015 Immune Checkpoint Blockade in Cancer Therapy. J Clin Oncol 33: 1974–82 [PubMed: 25605845]
3. Wang L, Rubinstein R, Lines JL, Wasiuk A, Ahonen C, Guo Y, Lu LF, Gondek D, Wang Y, Fava RA, Fiser A, Almo S, Noelle RJ. 2011 VISTA, a novel mouse Ig superfamily ligand that negatively regulates T cell responses. J Exp Med 208: 577–92 [PubMed: 21383057]
4. Xu W, Hieu T, Malarkannan S, Wang L. 2018 The structure, expression, and multifaceted role of immune-checkpoint protein VISTA as a critical regulator of anti-tumor immunity, autoimmunity, and inflammation. Cell Mol Immunol 15: 438–46 [PubMed: 29375120]
5. Flies DB, Wang S, Xu H, Chen L. 2011 Cutting edge: A monoclonal antibody specific for the programmed death-1 homolog prevents graft-versus-host disease in mouse models. J Immunol 187: 1537–41 [PubMed: 21768399]
6. Teft WA, Kirchhof MG, Madrenas J. 2006 A molecular perspective of CTLA-4 function. Annu Rev Immunol 24: 65–97 [PubMed: 16551244]
7. Hui E, Cheung J, Zhu J, Su X, Taylor MJ, Wallweber HA, Sasmal DK, Huang J, Kim JM, Mellman I, Vale RD. 2017 T cell costimulatory receptor CD28 is a primary target for PD-1-mediated inhibition. Science 355: 1428–33 [PubMed: 28280247]
8. Li N, Xu W, Yuan Y, Ayithan N, Imai Y, Wu X, Miller H, Olson M, Feng Y, Huang YH, Jo Turk M, Hwang ST, Malarkannan S, Wang L. 2017 Immune-checkpoint protein VISTA critically regulates the IL-23/IL-17 inflammatory axis. Scientific Reports 7: 1485 [PubMed: 28469254]
9. Flies DB, Han X, Higuchi T, Zheng L, Sun J, Ye JJ, Chen L. 2014 Coinhibitory receptor PD-1H preferentially suppresses CD4(+) T cell-mediated immunity. J Clin Invest 124: 1966–75 [PubMed: 24743150]

10. Wang L, Le Mercier I, Putra J, Chen W, Liu J, Schenk AD, Nowak EC, Suriawinata AA, Li J, Noelle RJ. 2014 Disruption of the immune-checkpoint VISTA gene imparts a proinflammatory phenotype with predisposition to the development of autoimmunity. Proc Natl Acad Sci U S A 111: 14846–51 [PubMed: 25267631]
11. Ceeraz S, Sergent PA, Plummer SF, Schned AR, Pechenick D, Burns CM, Noelle RJ. 2017 VISTA Deficiency Accelerates the Development of Fatal Murine Lupus Nephritis. Arthritis Rheumatol 69: 814–25 [PubMed: 27992697]
12. Le Mercier I, Chen W, Lines JL, Day M, Li J, Sergent P, Noelle RJ, Wang L. 2014 VISTA Regulates the Development of Protective Antitumor Immunity. Cancer Res 74: 1933–44 [PubMed: 24691994]
13. Liu J, Yuan Y, Chen W, Putra J, Suriawinata AA, Schenk AD, Miller HE, Guleria I, Barth RJ, Huang YH, Wang L. 2015 Immune-checkpoint proteins VISTA and PD-1 nonredundantly regulate murine T-cell responses. Proc Natl Acad Sci U S A 112: 6682–7 [PubMed: 25964334]
14. Lim KL, Chew KC, Tan JM, Wang C, Chung KK, Zhang Y, Tanaka Y, Smith W, Engelender S, Ross CA, Dawson VL, Dawson TM. 2005 Parkin mediates nonclassical, proteasomal-independent ubiquitination of synphilin-1: implications for Lewy body formation. J Neurosci 25: 2002–9 [PubMed: 15728840]
15. Chen Y, Zheng Y, You X, Yu M, Fu G, Su X, Zhou F, Zhu W, Wu Z, Zhang J, Wen R, Wang D. 2016 Kras Is Critical for B Cell Lymphopoiesis. J Immunol 196: 1678–85 [PubMed: 26773157]
16. Ahonen CL, Wasiuk A, Fuse S, Turk MJ, Ernstoff MS, Suriawinata AA, Gorham JD, Kedl RM, Usherwood EJ, Noelle RJ. 2008 Enhanced efficacy and reduced toxicity of multifactorial adjuvants compared with unitary adjuvants as cancer vaccines. Blood 111: 3116–25 [PubMed: 18202224]
17. Kawasaki T, Kawai T. 2014 Toll-like receptor signaling pathways. Front Immunol 5: 461 [PubMed: 25309543]
18. Janeway CA Jr., Medzhitov R 2002 Innate immune recognition. Annu Rev Immunol 20: 197–216 [PubMed: 11861602]
19. Liu W, Ouyang X, Yang J, Liu J, Li Q, Gu Y, Fukata M, Lin T, He JC, Abreu M, Unkeless JC, Mayer L, Xiong H. 2009 AP-1 activated by toll-like receptors regulates expression of IL-23 p19. J Biol Chem 284: 24006–16 [PubMed: 19592489]
20. Whitmarsh AJ. 2007 Regulation of gene transcription by mitogen-activated protein kinase signaling pathways. Biochim Biophys Acta 1773: 1285–98 [PubMed: 17196680]
21. Napetschnig J, Wu H. 2013 Molecular basis of NF-kappaB signaling. Annu Rev Biophys 42: 443–68 [PubMed: 23495970]
22. Takeda K, Kaisho T, Akira S. 2003 Toll-like receptors. Annu Rev Immunol 21: 335–76 [PubMed: 12524386]
23. Jiang Z, Mak TW, Sen G, Li X. 2004 Toll-like receptor 3-mediated activation of NF-kappaB and IRF3 diverges at Toll-IL-1 receptor domain-containing adapter inducing IFN-beta. Proc Natl Acad Sci U S A 101: 3533–8 [PubMed: 14982987]
24. Kawai T, Akira S. 2010 The role of pattern-recognition receptors in innate immunity: update on Toll-like receptors. Nat Immunol 11: 373–84 [PubMed: 20404851]
25. Adhikari A, Xu M, Chen ZJ. 2007 Ubiquitin-mediated activation of TAK1 and IKK. Oncogene 26: 3214–26 [PubMed: 17496917]
26. Lu H 2014 TLR Agonists for Cancer Immunotherapy: Tipping the Balance between the Immune Stimulatory and Inhibitory Effects. Front Immunol 5: 83 [PubMed: 24624132]
27. Dowling JK, Mansell A. 2016 Toll-like receptors: the swiss army knife of immunity and vaccine development. Clin Transl Immunology 5: e85 [PubMed: 27350884]
28. Kumar V, Patel S, Tcyganov E, Gabrilovich DI. 2016 The Nature of Myeloid-Derived Suppressor Cells in the Tumor Microenvironment. Trends Immunol 37: 208–20 [PubMed: 26858199]
29. Veglia F, Gabrilovich DI. 2017 Dendritic cells in cancer: the role revisited. Curr Opin Immunol 45: 43–51 [PubMed: 28192720]
30. Xu M, Mizoguchi I, Morishima N, Chiba Y, Mizuguchi J, Yoshimoto T. 2010. Regulation of antitumor immune responses by the IL-12 family cytokines, IL-12, IL-23, and IL-27. Clin Dev Immunol 2010

31. Spranger S, Dai D, Horton B, Gajewski TF. 2017 Tumor-Residing Batf3 Dendritic Cells Are Required for Effector T Cell Trafficking and Adoptive T Cell Therapy. Cancer Cell 31: 711–23 e4 [PubMed: 28486109]
32. Broz ML, Binnewies M, Boldajipour B, Nelson AE, Pollack JL, Erle DJ, Barczak A, Rosenblum MD, Daud A, Barber DL, Amigorena S, Van't Veer LJ, Sperling AI, Wolf DM, Krummel MF. 2014 Dissecting the Tumor Myeloid Compartment Reveals Rare Activating Antigen-Presenting Cells Critical for T Cell Immunity. Cancer Cell 26: 938
33. Lines JL, Pantazi E, Mak J, Sempere LF, Wang L, O'Connell S, Ceeraz S, Suriawinata AA, Yan S, Ernstoff MS, Noelle R. 2014 VISTA Is an Immune Checkpoint Molecule for Human T Cells. Cancer Res 74: 1924–32 [PubMed: 24691993]
34. Gao J, Ward JF, Pettaway CA, Shi LZ, Subudhi SK, Vence LM, Zhao H, Chen J, Chen H, Efstathiou E, Troncoso P, Allison JP, Logothetis CJ, Wistuba II, Sepulveda MA, Sun J, Wargo J, Blando J, Sharma P. 2017 VISTA is an inhibitory immune checkpoint that is increased after ipilimumab therapy in patients with prostate cancer. Nat Med 23: 551–5 [PubMed: 28346412]
35. Connolly DJ, O'Neill LA. 2012 New developments in Toll-like receptor targeted therapeutics. Curr Opin Pharmacol 12: 510–8 [PubMed: 22748800]
36. Marabelle A, Filatenkov A, Sagiv-Barfi I, Kohrt H. 2015 Radiotherapy and toll-like receptor agonists. Semin Radiat Oncol 25: 34–9 [PubMed: 25481264]
37. Goutagny N, Estornes Y, Hasan U, Lebecque S, Caux C. 2012 Targeting pattern recognition receptors in cancer immunotherapy. Target Oncol 7: 29–54 [PubMed: 22399234]
38. Groom JR, Luster AD. 2011 CXCR3 ligands: redundant, collaborative and antagonistic functions. Immunol Cell Biol 89: 207–15 [PubMed: 21221121]
39. Gonzalez-Martin A, Gomez L, Lustgarten J, Mira E, Manes S. 2011 Maximal T cell-mediated antitumor responses rely upon CCR5 expression in both CD4(+) and CD8(+) T cells. Cancer Res 71: 5455–66 [PubMed: 21715565]
40. Liu JY, Li F, Wang LP, Chen XF, Wang D, Cao L, Ping Y, Zhao S, Li B, Thorne SH, Zhang B, Kalinski P, Zhang Y. 2015 CTL- vs Treg lymphocyte-attracting chemokines, CCL4 and CCL20, are strong reciprocal predictive markers for survival of patients with oesophageal squamous cell carcinoma. Br J Cancer 113: 747–55 [PubMed: 26284335]
41. Murugaiyan G, Saha B. 2013 IL-27 in tumor immunity and immunotherapy. Trends Mol Med 19: 108–16 [PubMed: 23306374]
42. Corrales L, Matson V, Flood B, Spranger S, Gajewski TF. 2017 Innate immune signaling and regulation in cancer immunotherapy. Cell Res 27: 96–108 [PubMed: 27981969]
43. Bromberg J, Wang TC. 2009 Inflammation and cancer: IL-6 and STAT3 complete the link. Cancer Cell 15: 79–80 [PubMed: 19185839]
44. Teng MW, Bowman EP, McElwee JJ, Smyth MJ, Casanova JL, Cooper AM, Cua DJ. 2015 IL-12 and IL-23 cytokines: from discovery to targeted therapies for immune-mediated inflammatory diseases. Nat Med 21: 719–29 [PubMed: 26121196]
45. Veglia F, Perego M, Gabrilovich D. 2018 Myeloid-derived suppressor cells coming of age. Nat Immunol 19: 108–19 [PubMed: 29348500]
46. Curiel TJ, Wei S, Dong H, Alvarez X, Cheng P, Mottram P, Krzysiek R, Knutson KL, Daniel B, Zimmermann MC, David O, Burow M, Gordon A, Dhurandhar N, Myers L, Berggren R, Hemminki A, Alvarez RD, Emilie D, Curiel DT, Chen L, Zou W. 2003 Blockade of B7-H1 improves myeloid dendritic cell-mediated antitumor immunity. Nat Med 9: 562–7 [PubMed: 12704383]
47. Tesone AJ, Rutkowski MR, Brencicova E, Svoronos N, Perales-Puchalt A, Stephen TL, Allegrezza MJ, Payne KK, Nguyen JM, Wickramasinghe J, Tchou J, Borowsky ME, Rabinovich GA, Kossenkov AV, Conejo-Garcia JR. 2016 Satb1 Overexpression Drives Tumor-Promoting Activities in Cancer-Associated Dendritic Cells. Cell Rep 14: 1774–86 [PubMed: 26876172]
48. Weber R, Fleming V, Hu X, Nagibin V, Groth C, Altevogt P, Utikal J, Umansky V. 2018 Myeloid-Derived Suppressor Cells Hinder the Anti-Cancer Activity of Immune Checkpoint Inhibitors. Front Immunol 9: 1310 [PubMed: 29942309]
49. Tsujikawa T, Kumar S, Borkar RN, Azimi V, Thibault G, Chang YH, Balter A, Kawashima R, Choe G, Sauer D, El Rassi E, Clayburgh DR, Kulesz-Martin MF, Lutz ER, Zheng L, Jaffee EM,

Leyshock P, Margolin AA, Mori M, Gray JW, Flint PW, Coussens LM. 2017 Quantitative Multiplex Immunohistochemistry Reveals Myeloid-Inflamed Tumor-Immune Complexity Associated with Poor Prognosis. Cell Rep 19: 203–17 [PubMed: 28380359]

50. Serafini P, Meckel K, Kelso M, Noonan K, Califano J, Koch W, Dolcetti L, Bronte V, Borrello I. 2006 Phosphodiesterase-5 inhibition augments endogenous antitumor immunity by reducing myeloid-derived suppressor cell function. J Exp Med 203: 2691–702 [PubMed: 17101732]
51. Clark CE, Hingorani SR, Mick R, Combs C, Tuveson DA, Vonderheide RH. 2007 Dynamics of the immune reaction to pancreatic cancer from inception to invasion. Cancer Res 67: 9518–27 [PubMed: 17909062]
52. Kim K, Skora AD, Li Z, Liu Q, Tam AJ, Blosser RL, Diaz LA Jr., Papadopoulos N, Kinzler KW, Vogelstein B, Zhou S. 2014 Eradication of metastatic mouse cancers resistant to immune checkpoint blockade by suppression of myeloid-derived cells. Proc Natl Acad Sci U S A 111: 11774–9 [PubMed: 25071169]
53. Davis RJ, Moore EC, Clavijo PE, Friedman J, Cash H, Chen Z, Silvin C, Van Waes C, Allen C. 2017 Anti-PD-L1 Efficacy Can Be Enhanced by Inhibition of Myeloid-Derived Suppressor Cells with a Selective Inhibitor of PI3Kdelta/gamma. Cancer Res 77: 2607–19 [PubMed: 28364000]

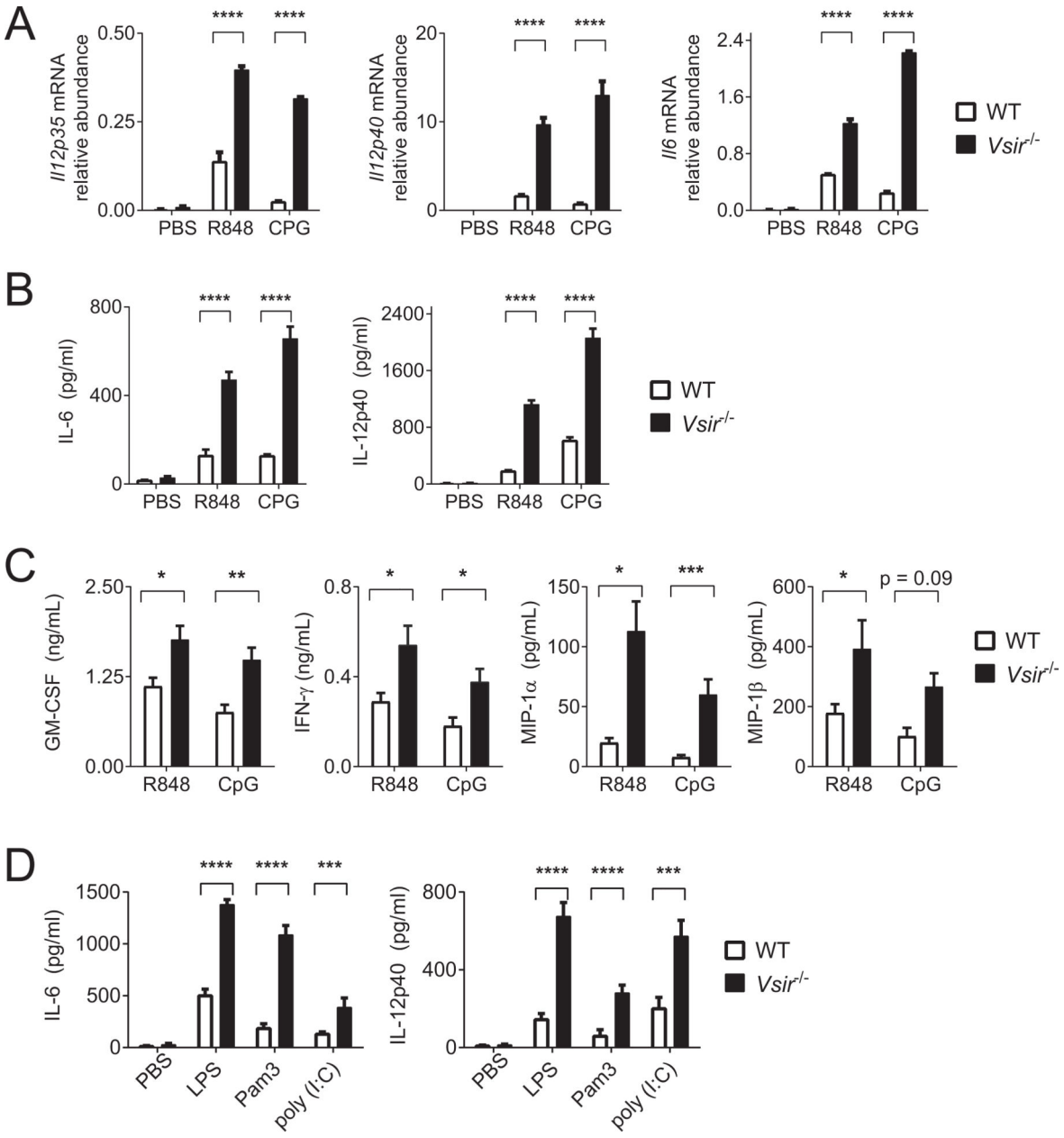

Figure 1: Genetic deletion of VISTA augments the expression of inflammatory cytokines in macrophages in response to TLR stimulation.

(A-C) WT and *Vsir*$^{-/-}$ peritoneal macrophages were isolated and pooled from three mice of each genotype. Cells were stimulated *ex vivo* with PBS, R848 (5 μg/mL; TLR7/8), and CpG (1 μg/mL; TLR9). RNA was extracted and supernatants were collected after 3 hours and 6 hours of culture, respectively. (A) Gene expression of *Il12p35*, *Il12p40*, and *Il6* was examined by real-time qRT-PCR. (B) Secreted IL12p40 and IL6 were examined by ELISA. (C) Additional cytokines (GM-CSF and IFNγ) and chemokines (MIP-1α and MIP-1β) were also examined by ELISA. (D) WT and *Vsir*$^{-/-}$ macrophages were stimulated with TLR agonists LPS (1 μg/mL; TLR4), Pam3Cys4 (Pam3, 10μg/mL; TLR2), and poly (I:C)(25 μg/mL; TLR3) for 6 hours. Secreted IL6 and IL12p40 were quantified by ELISA. Statistical

significance was determined by unpaired two-tailed t test. Error bars indicate the standard error of the mean (SEM). *p<0.05; **p<0.01; ***p<0.001; ****p<0.0001. Shown are representative results from at least three independent repeats.

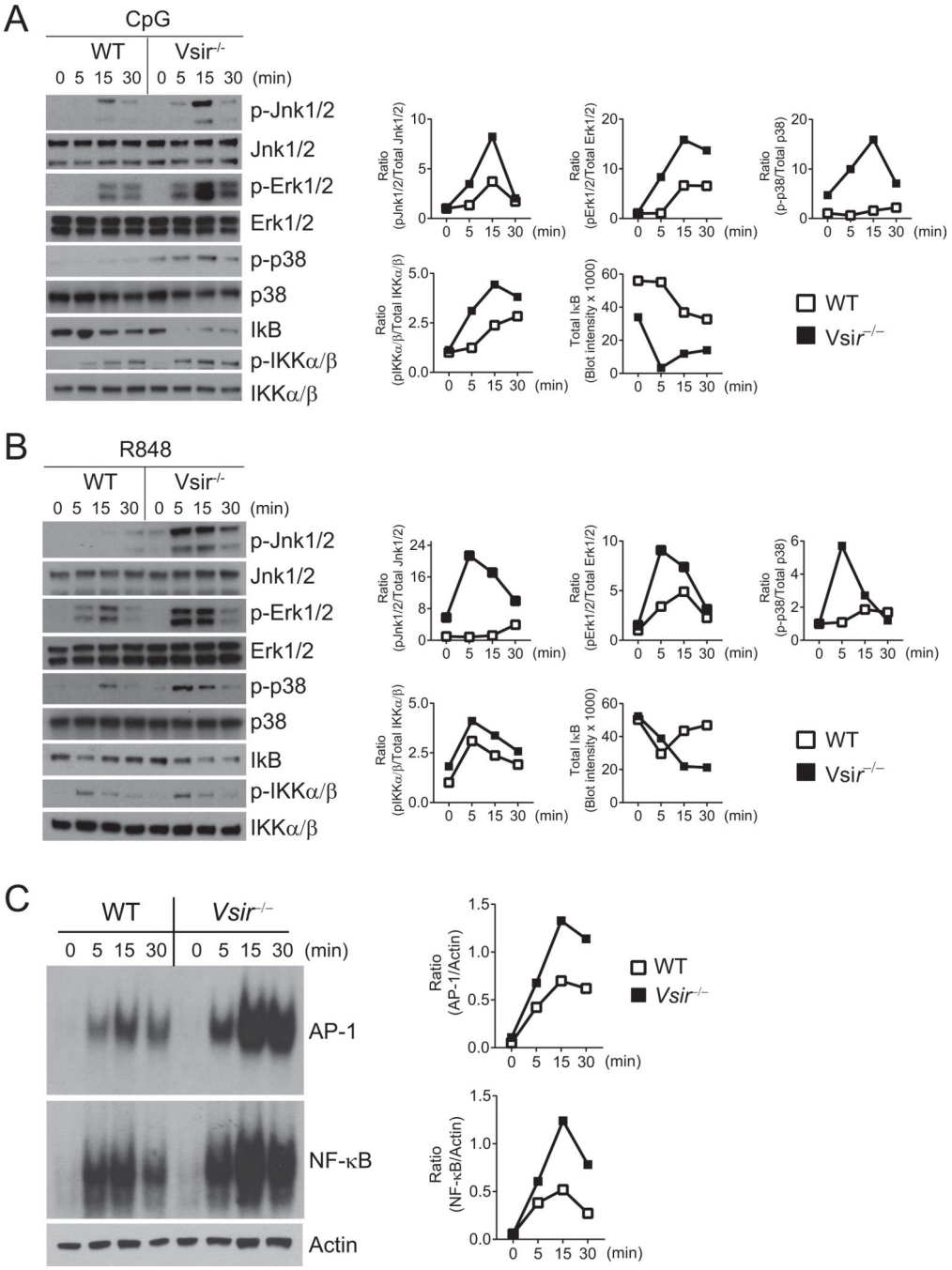

Figure 2: Genetic deletion of VISTA enhances the activation of MAPKs/AP-1 and IKKα/β/NF-κB pathways following TLR7 and TLR9 stimulation.

WT and *Vsir*$^{-/-}$ peritoneal macrophages pooled from two-three mice of each genotype were stimulated with (A) CpG (1 μg/mL) or (B) R848 (10 μg/mL) for the indicated amount of time before total cell lysates were assessed. Phosphorylated (p-) and total Jnk1/2, Erk1/2, p38, and IKKα/β, and total IκB were examined by Western blotting and quantified using Image J software.Ratios of phosphorylated vs. total protein were shown. (C) WT and *Vsir*$^{-/-}$ peritoneal macrophages were stimulated with CpG (1 μg/mL) as indicated. DNA binding activity of AP-1 and NF-κB in total cell lysates was measured using an EMSA assay and

visualized by autoradiography. Actin in the total lysates were determined by Western blotting. The amount of bound probes was normalized to actin in the total lysates. Shown are representative results from at least three independent repeats.

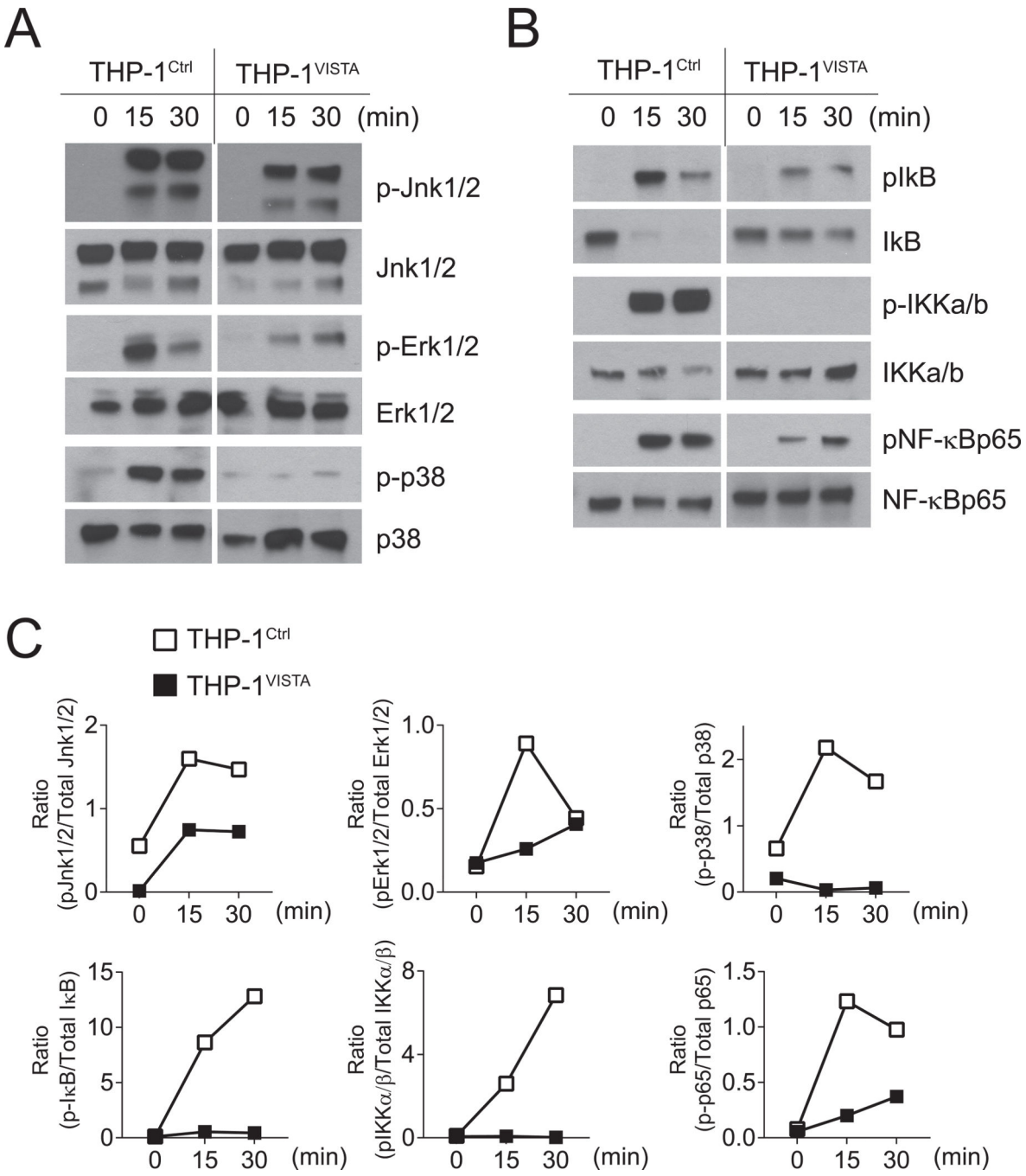

Figure 3: VISTA overexpression in human monocyte THP-1 cells inhibits the activation of MAPKs and NF-κB following TLR2 stimulation.

Human monocyte THP-1 cells overexpressing VISTA (THP-1^{VISTA}) and control cells (THP-1^{Ctrl}) were stimulated with Pam3Cys4 (10 μg/mL) for the indicated amount of time. (A-B) Total cell lysates were generated and examined by Western blotting. Phosphorylated (p-) Jnk1/2, Erk1/2, p38, IKKα/β, and NF-κBp65, and total IκB were quantified by Image J software and shown in panel C. Shown are representative results from at least three independent repeats.

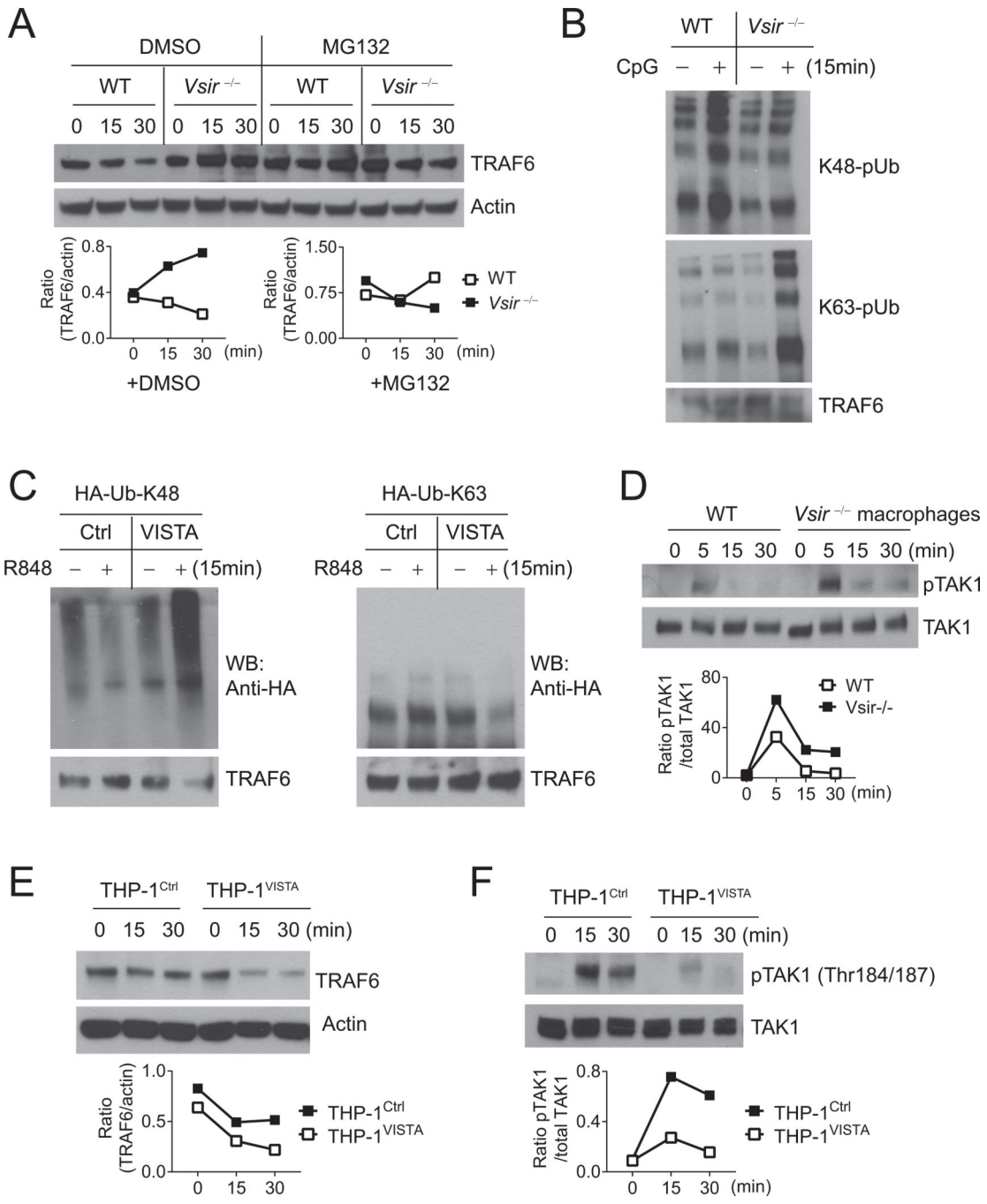

Figure 4: VISTA modulates the K48-linked and K63-linked polyubiquitination of TRAF6 and inhibits the activation of TAK1 following TLR stimulation.

(A) WT and *Vsir*$^{-/-}$ peritoneal macrophages (pooled from two to three mice of each genotype) were pretreated with MG132 (10μg/mL) or vehicle control DMSO for 30 minutes before being stimulated with CpG (1 μg/mL) for 0, 15, and 30 minutes. TRAF6 and actin in total cell lysates were determined by Western blotting. (B) To examine the ubiquitination status, WT and *Vsir*$^{-/-}$ peritoneal macrophages (pooled from two to three mice of each genotype) were stimulated with CpG (1 μg/mL) for 15 minutes. TRAF6 protein was immunoprecipitated from total lysates under denaturing conditions. K63-linked and K48-

linked polyubiquitination (pUb) were examined by Western blotting using antibodies specific for K48-linked or K63-linked polyubiquitin chains. (C) TLR7-expressing HEK293T cells were transfected with HA-tagged mutant ubiquitin HA-Ub-K48 or HA-Ub-K63, together with a VISTA-expressing plasmid or vector control as indicated. Cells were stimulated with R848 at 24 hours post transfection. TRAF6 was immunoprecipitated as in (B) and examined by Western blotting (WB) using anti-HA. (D) WT and *Vsir*$^{-/-}$ peritoneal macrophages were stimulated by CpG (1 μg/mL) for indicated amount of time. Phosphorylated (p-) and total TAK1 in cell lysates were examined by Western blotting and quantified using Image J software. The ratio of pTAK1/TAK1 was shown. (E,F) VISTA-expressing THP-1 cells (THP-1^{VISTA}) and control cells (THP-1^{Ctrl}) were stimulated with Pam3Cys4 (10 μg/mL) for indicated amount of time. TRAF6, actin, pTAK1, and total TAK1 in total cell lysates were examined by Western blotting and quantified using Image J. Ratios of TRAF6/actin and pTAK1/TAK1 were shown. Shown are representative results from at least three independent repeats.

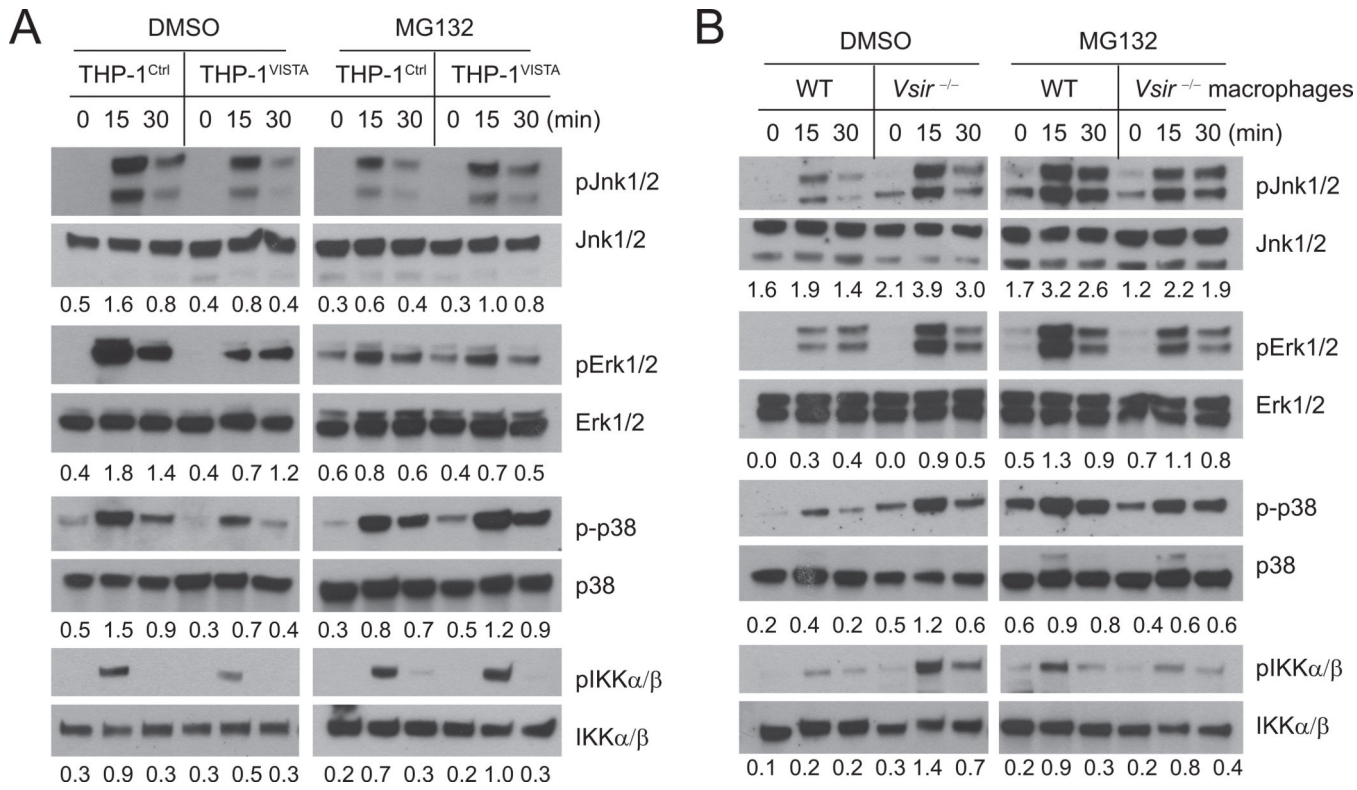

Figure 5: The proteasome inhibitor MG132 reverses the inhibitory effect of VISTA on TLR signaling.

(A) VISTA-expressing THP-1 cells (THP-1^{VISTA}) and control cells (THP-1^{Ctrl}) were pretreated with DMSO solvent control or MG132 (10 μg/mL) for 30 minutes prior to stimulation with Pam3Cys4 (10 μg/mL). Phosphorylation (p) of Jnk1/2, Erk1/2, TAK1, and IKKα/β were examined by Western blotting. The ratios of phosphorylated proteins to total protein were quantified using Image J software and shown numerically under each time point. (B) WT and *Vsir*$^{-/-}$ peritoneal macrophages (pooled from two-three mice of each genotype) were pretreated with DMSO or MG132 as in A before being stimulated with CpG (1 μg/mL). Total lysates were generated and analyzed as in A. Shown are representative results from three independent repeats.

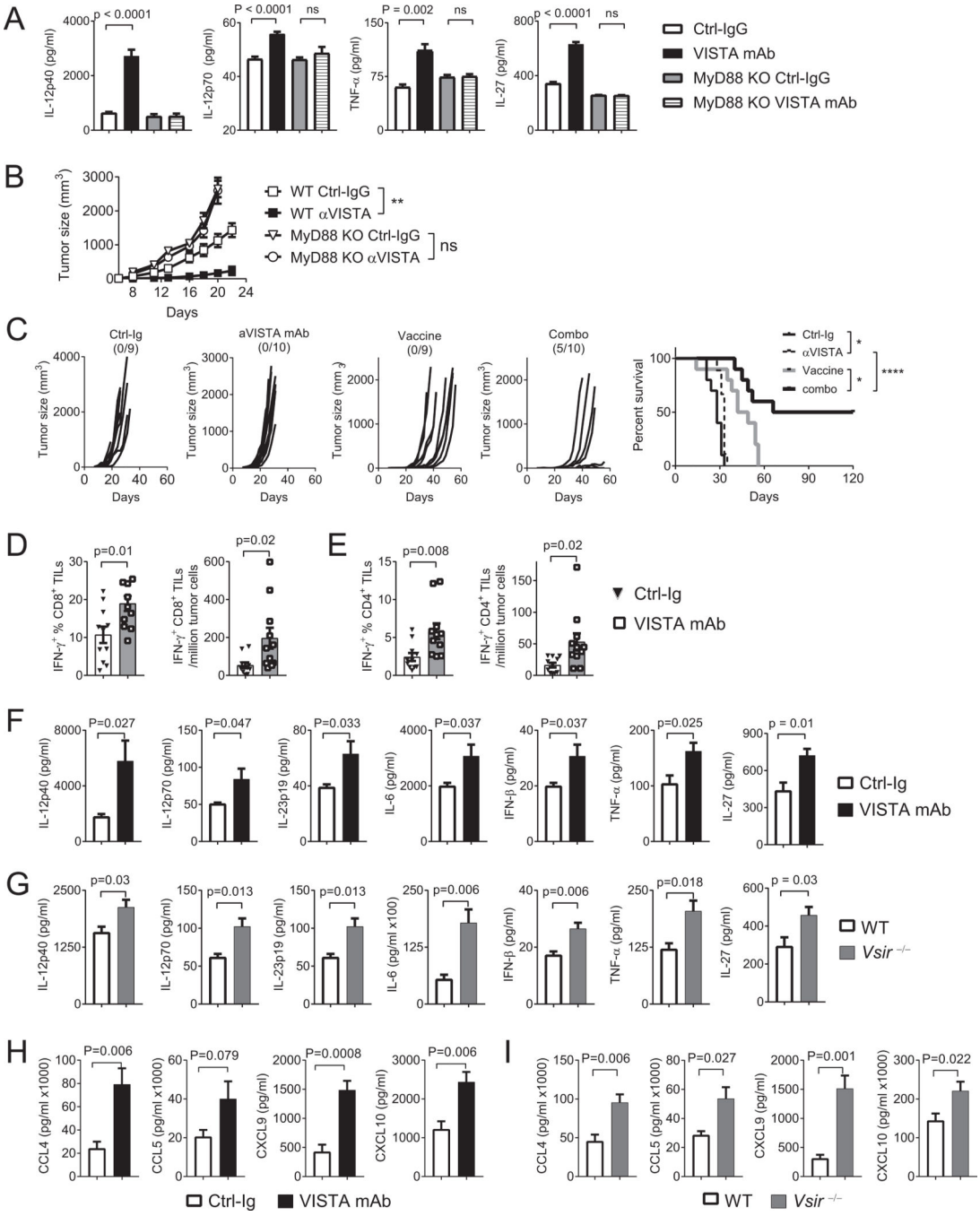

Figure 6: TLR/MyD88-mediated inflammation promotes the therapeutic efficacy of VISTA blockade.

(A) WT or MyD88 KO mice were inoculated with B16-BL6 melanoma cells (200,000) on the flank on day 0. On day +7 mice bearing established tumors (~5 mm in diameter) were treated with VISTA-blocking mAb or isotype control IgG (n=10/group). Three hours later, serum was harvested and examined by ELISA for cytokines. (B) WT and MyD88 KO mice (n=6–7/group) were inoculated with EG7 thymoma cells (150,000). Beginning on day 2 and repeated every 2–3 days, tumor-bearing mice were treated with VISTA-blocking mAb or control IgG. Tumor size was measured by a caliper. Shown are representative results from

three independent repeats. (C-E) Naïve WT mice (n=10) were inoculated with B16-BL6 melanoma cells (30,000) on day 0. On day +3, tumor-bearing mice were treated with a peptide vaccine containing CpG, R848, and peptides (details in Methods). Mice were also treated with VISTA-blocking mAb or control IgG every 2–3 days. (C) Tumor size was recorded. In a separate group of mice (n=10), tumor tissues (~6–8 mm in diameter) were harvested. Tumor-infiltrating $CD4^+$ and $CD8^+$ T cells were stimulated with anti-CD3. Percentage and number of IFNγ-expressing (D) $CD8^+$ T cells and (E) $CD4^+$ T cells were examined by flow cytometry. (F,H) To examine the inflammatory TME, we treated B16-BL6 tumor-bearing mice (n= 5–7/group) with the peptide vaccine and VISTA-blocking mAb or control IgG. Tumor tissues were harvested after three hours and homogenized. Cytokines (IL12p40, IL12p70, IL23p19, IL6, TNFα, and IFNβ) and chemokines (CCL4, CCL5, CXCL9, CXCL10) in the homogenates were quantified by ELISA. (G,I) B16-BL6 tumors were harvested from WT and *Vsir*$^{-/-}$ mice (n=5–7/group) following treatment with the peptide vaccine as described above. Cytokines and chemokines in tumor tissue homogenates were examined by ELISA. Statistical significance of all results was determined by unpaired two-tailed t test. Error bars represent SEM. *p<0.05; **p<0.01; ***p<0.001; ****p<0.0001. Shown are representative results from three independent repeats.

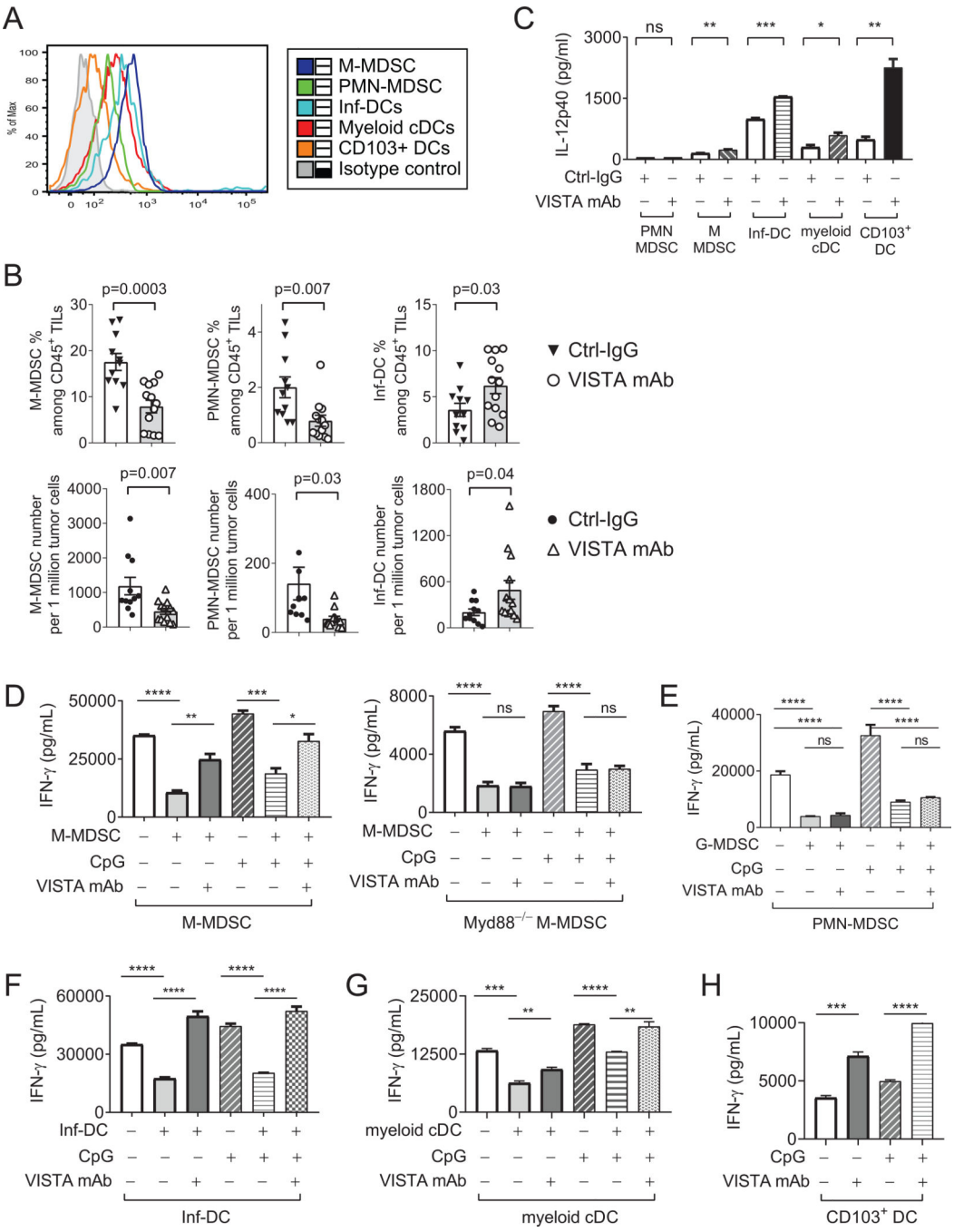

Figure 7: VISTA regulates the accumulation and effector functions of tumor-associated MDSCs and DC subsets.

(A) Tumor tissues were harvested from five B16-BL6 tumor-bearing mice and pooled. VISTA expression on tumor-infiltrating MDSCs and DC subsets were examined by flow cytometry.(B) Mice bearing established B16-BL6 tumors (4–5 mm in diameter) were treated with TLR agonists CpG and R848 together with the VISTA-blocking mAb or isotype control IgG. Numbers of tumor-infiltrating M-MDSCs, PMN-MDSCs, and Inf-DCs were examined by flow cytometry 48 hours post treatment. P values shown. (C) Tumor-associated PMN-MDSCs, M-MDSCs, myeloid cDCs, Inf-DCs, and CD103^{+} DCs were sorted from

pooled B16-BL6 tumor tissues (7–8 mm in diameter) harvested from twenty to thirty tumor-bearing mice. Each type of purified myeloid cells (10,000 cells each) were stimulated *ex vivo* with CpG (1 μg/mL) in the presence of VISTA blocking mAb or control IgG. Culture supernatants were collected after 24 hours and and IL12p40 were quantified by ELISA. (D) M-MDSCs (WT and MyD88 KO), (E) PMN-MDSCs, (F) Inf-DCs, and (G) myeloid cDCs were sorted from B16-BL6 tumor tissues (pooled from twenty – thirty tumor-bearing mice) and cocultured with whole splenocytes from the OT-I transgenic mice in the presence of OVA peptide. CpG and VISTA-blocking mAb or control IgG were added as indicated. Culture supernatants were harvested after 48 hours and IFNγ was examined by ELISA. (H) Tumor-associated $CD103^+$ DCs were sorted from B16-BL6 tumor tissues and incubated with purified naïve OT-I $CD8^+$ T cells in the presence of OVA peptide and VISTA-blocking mAb or control IgG. After 48 hours, secreted IFNγ was examined by ELISA. Statistical significance of all results was determined by unpaired two-tailed t test. Error bars represent SEM. *p<0.05; **p<0.01; ***p<0.001; ****p<0.0001. Results from three independent experiments were shown.